e-ISSN: 2687-6698 Research Article

Turkish Journal of Analytical Chemistry

TurkJAC

https://dergipark.org.tr/tr/pub/turkjac

Eco-friendly spectrofluorimetric determination of Hg^{2+} using green-synthesized carbon nanodots from apricot kernel shells

Najlaa Ayad Salahaldeen[1], Nurhayat Özbek[1], Miraç Ocak[1]*, Ümmühan Turgut Ocak[1]

[1] Karadeniz Technical University, Faculty of Sciences, Department of Chemistry, 61080, Trabzon, Türkiye

Abstract

The green synthesis of blue fluorescent carbon nanodots (CNDs) from apricot kernel shells via a hydrothermal method was successfully executed. The interaction of the synthesized CNDs with various cations was systematically investigated using fluorescence spectroscopy. Fluorescence measurements were performed to evaluate the interaction of CNDs with 36 different cations, including Li^{+}, Na^{+}, K^{+}, Be^{2+}, Mg^{2+}, Ca^{2+}, Sr^{2+}, Ba^{2+}, Sc^{3+}, Y^{3+}, Ti^{4+}, V^{5+}, Cr^{3+}, Mo^{6+}, W^{6+}, Mn^{2+}, Fe^{3+}, Co^{2+}, Ni^{2+}, Cu^{2+}, Ag^{+}, Zn^{2+}, Cd^{2+}, B^{3+}, Al^{3+}, Tl^{+}, As^{5+}, Se^{2+}, NH_4^{+}, Au^{3+}, Sb^{3+}, Sn^{4+}, Bi^{3+}, Hg^{2+}, Pd^{2+}, and Pb^{2+}. Among these, the CNDs exhibited exceptional selectivity and sensitivity as a fluorescent probe for the detection of Hg^{2+} ions. The working range for Hg^{2+} detection was established as 35–95 µM, with a detection limit of 14.0 µM and a quantification limit of 41.4 µM. The method was validated and successfully applied to tap water and river water, demonstrating the practical utility of CNDs derived from apricot seed shells for environmental monitoring and analytical applications.

Keywords: Carbon nanodots (CNDs), hydrothermal method, apricot kernel shell, fluorescence spectroscopy, Hg^{2+} determination.

1. Introduction

CNDs, a class of carbon-based nanomaterials, have garnered significant attention in recent years due to their unique optical properties, biocompatibility, environmental friendliness, and cost-effective synthesis [1-2]. These nanomaterials exhibit high fluorescence quantum yields, excellent photostability, and versatile surface functionalization capabilities, making them ideal candidates for sensing applications, especially in fluorescence-based detection systems [3-4]. Among these, the detection of heavy metal ions, particularly Hg^{2+}, has been a major focus due to its toxicological and environmental significance [5].

Mercury is a highly toxic heavy metal with severe impacts on human health and ecosystems even at trace levels [6]. It is well known for its bioaccumulation in the food chain and persistence in the environment [7]. Consequently, the development of efficient, sensitive, and selective methods for Hg^{2+} detection has become a pressing need. In this context, CNDs-based spectrofluorimetric techniques have emerged as promising tools, offering rapid, cost-effective, and environmentally friendly solutions for mercury ion detection.

Numerous studies in the literature highlight the potential of CNDs for Hg^{2+} sensing, leveraging their remarkable fluorescence properties and unique interaction mechanisms [8]. The fluorescence quenching of CNDs in the presence of Hg^{2+} is a commonly employed detection strategy, attributed to processes such as static or dynamic quenching [9-12]. The strong affinity of Hg^{2+} ions for the functional groups on the surface of CNDs, such as carboxyl, hydroxyl, or amine groups, underpins the high sensitivity and selectivity of these systems [13].

Significant advancements have been reported in the development of CND-based sensors with ultra-low detection limits, often reaching nanomolar or even picomolar levels [14-15]. These sensors have demonstrated excellent selectivity for Hg^{2+} over other metal ions, making them suitable for applications in environmental water samples [16-17]. Additionally, the use of green synthesis approaches for producing CNDs from natural or waste-derived carbon sources has

Citation: N. A. Salahaldeen, N. Özbek, M. Ocak, Ü.T. Ocak, Eco-friendly spectrofluorimetric determination of Hg^{2+} using green-synthesized carbon nanodots from apricot kernel shells, Turk J Anal Chem, 7(2), 2025, 228–236.

***Author of correspondence:** mocak@ktu.edu.tr
Tel: +90 (462) 377 25 25 **Fax:** +90 (462) 325 31 96

Received: March 16, 2025 **Accepted:** April 23, 2025
https://doi.org/10.51435/turkjac.1658256

further enhanced their appeal as sustainable materials for analytical applications [18-19].

Recent studies have explored the synthesis of CNDs from apricot kernel shells, highlighting their potential in various applications. For instance, Xu et al. utilized a carbonization technique to produce greenish-yellow luminescent carbon quantum dots from apricot shells, demonstrating high photostability [20]. Another study focused on the preparation and characterization of biochar derived from apricot kernel shells using a hydrothermal method. The resulting biochar exhibited a uniform distribution of non-aggregated carbon microspheres and contained numerous oxygen-containing functional groups, indicating its potential for adsorption applications [21]. Additionally, research has been conducted on recycling lignocellulosic waste, including apricot kernels, to design advanced carbon material precursors. These precursors can be used to obtain nanopowders with high applicability in pollution abatement, showcasing the versatility of apricot kernel-derived carbon materials [22].

Although there is extensive research on the use of biomass-derived CNDs for the spectrofluorimetric detection of metal ions [23], studies specifically focused on metal ion determination using CNDs derived from apricot kernel shells remain highly limited in the literature [20]. In a recent study, greenish-yellow fluorescent carbon quantum dots synthesized from apricot kernel shells exhibited selective fluorescence quenching in the presence of Fe^{3+} ions, with the fluorescence being restored upon the addition of ascorbic acid [20]. This finding demonstrated the potential of these CNDs for the selective detection of ascorbic acid [20].

In the presented study, CNDs were synthesized using a simple and rapid hydrothermal method from apricot kernel shells, and their interactions with a series of cations were investigated through fluorescence measurements. Among the examined cations, selective fluorescence quenching was observed with Be^{2+}, V^{5+}, Fe^{3+}, Au^{3+}, Hg^{2+}, and Pd^{2+} ions. Notably, the fluorescence quenching of CNDs was found to be linearly dependent on Hg^{2+} ion concentration, making it possible to develop a new spectrofluorimetric method for the detection of Hg^{2+}. The applicability of this method to real samples was also demonstrated. Thus, the presented study addresses a gap in the literature by providing a simple, rapid, and cost-effective spectrofluorimetric method for the determination of Hg^{2+} using CNDs synthesized from apricot kernel shells.

2. Materials and Methods

2.1. Instrumentation, reagents, and samples

The instrumentation employed in this study included a Photon Technologies International Quanta Master Spectrofluorimeter (QM-4-2006) for fluorescence measurements, a high-precision Sartorius Ed224s analytical balance for mass determination, and an Analytik Jena Specord 210 spectrophotometer for UV-Vis absorption spectroscopy. Sample preparation was conducted using a Vacuell Eco Line vacuum oven, a HERMLE Z 326 K centrifuge, an IKA RCT magnetic stirrer, and a JSOF-050 forced convection oven. Sample mixing and volumetric handling were facilitated by a Labnet Model No. 50100-320 V vortex shaker and Nichiryo automatic pipettes (10-100-1000 µL). Deionized water used in the study was obtained from a Merck Millipore Direct-Q 8 UV system. Ultraviolet measurements were performed using a SPECTROLINE MODEL CM-10 UV device, while pH analyses were carried out with an Orion Research Model 601 Digital Ionalyzer pH meter. Dialysis bags (6000 Da) were obtained from Merck (Darmstadt, Germany). Single-use filters with a pore size of 0.45 microns were purchased from Sartorius. Standard aqueous solutions of cations (1000 mg/L) were supplied by Merck. The real water samples analyzed in this study were tap water from Karadeniz Technical University (KTU) and water from the Harşit River.

2.2. Preparation of the CNDs

The apricot kernels were carefully cleaned, dried, and finely ground using a laboratory grinder. A precisely measured 1.0 g of the powdered material was dispersed in 150 mL of deionized water. The resulting mixture underwent hydrothermal treatment in a stainless steel autoclave at 180°C for 3 hours. Upon completion of the reaction, the obtained solution was sequentially filtered through black and white band filter papers to eliminate solid residues. The filtrate was subsequently centrifuged at 10000 rpm for 10 minutes to further purify the suspension. The supernatant was then subjected to dialysis against 200 mL of deionized water under continuous stirring at 600 rpm for 3 days, utilizing a dialysis membrane with a molecular weight cut-off of 6000 Da. Following dialysis, the external solution was separately filtered through a 0.45-micron membrane filter to ensure the complete removal of any residual impurities. A 12.5 mL aliquot of the external solution was collected and diluted to a final volume of 100 mL with deionized water. The purified CND solution obtained after dialysis and filtration was subsequently diluted and utilized in spectrofluorimetric analyses for the detection of Hg^{2+} ions.

2.3. Determination of the quantum yield

The quantum yield of the synthesized CNDs (Φ_{CNDs}) was determined using a comparative method, as described in previous studies [24]. A 0.1 M solution of quinine sulfate in 0.1 M H_2SO_4 (Φ_R = 0.54) with a refractive index (η) of

1.33 served as the reference fluorescence standard. The CND solutions were prepared in deionized water, also with a refractive index (η) of 1.33, to ensure consistency in optical properties. Fluorescence emission spectra were recorded for both the quinine sulfate reference and the CND solutions at varying concentrations, with an excitation wavelength (λ_{ex}) of 310 nm. The integrated fluorescence intensity values of the emission spectra were calculated. Corresponding absorbance values for each solution were measured under the same conditions as the emission spectra to maintain accuracy. A linear plot of integrated fluorescence intensity versus absorbance was generated for both the reference and the CND solutions. The slope (m) of the linear fit for the CNDs was compared to that of the reference solution, enabling calculation of the quantum yield for the CNDs using Eq. 1.

$$\Phi_{\text{CNDs}} = \Phi_Q \left(\frac{m_{CNDs}}{m_Q}\right)\left(\frac{\eta^2_{\text{CNDs}}}{\eta^2_Q}\right) \quad (1)$$

In Equation (1), the terms CNDs and Q represent the synthesized CNDs and quinine sulfate, respectively. The parameter m corresponds to the slope obtained from the linear plot of integrated fluorescence intensity versus absorbance for each solution. The refractive index, η, represents the optical property of the solvent used for each sample, accounting for variations in the medium's influence on fluorescence efficiency. These parameters collectively enable accurate determination of the quantum yield of CNDs relative to the reference standard.

2.4. pH effect on the fluorescence spectra of CNDs

To investigate the effect of pH on the fluorescence intensity of the CNDs, solutions were prepared across a pH range of 3 to 11 using appropriate buffer systems to maintain pH stability. Fluorescence measurements were performed by exciting the CND solutions at a wavelength of 310 nm, and the corresponding emission intensities were recorded. This systematic study was conducted to evaluate the impact of pH on the photophysical properties of the CNDs.

2.5. Interactions of cations with CNDs

2 mL of the CND solution was aliquoted into separate tubes. To achieve a final cation concentration of 1×10^{-3} M, appropriate volumes of the prepared intermediate stock solutions were added. The total volume in each tube was adjusted to 4 mL by adding deionized water. The fluorescence spectra of the prepared samples were then recorded, with excitation set at the wavelength corresponding to the maximum fluorescence intensity of the CNDs. The interactions of CNDs with cations such as Li^+, Na^+, K^+, Be^{2+}, Mg^{2+}, Ca^{2+}, Sr^{2+}, Ba^{2+}, Sc^{3+}, Y^{3+}, Ti^{4+}, V^{5+}, Cr^{3+}, Mo^{6+}, W^{6+}, Mn^{2+}, Fe^{3+}, Co^{2+}, Ni^{2+}, Cu^{2+}, Ag^+, Zn^{2+}, Cd^{2+}, B^{3+}, Al^{3+}, Tl^+, As^{5+}, Se^{2+}, NH_4^+, Au^{3+}, Sb^{3+}, Sn^{4+}, Bi^{3+}, Hg^{2+}, Pd^{2+}, and Pb^{2+} were investigated spectrofluorimetrically. Among these, a regular decrease in fluorescence intensity was observed during titrations with increasing concentrations of Hg^{2+} ions, indicating a selective quenching effect.

2.6. Determination of Hg^{2+} ions

A spectrofluorimetric method for the determination of Hg^{2+} was developed based on the regular fluorescence quenching exhibited by CNDs in the presence of Hg^{2+}. Initially, Hg^{2+} was added to pure water to calculate the recovery values. For this, a standard calibration curve was prepared and used to determine the concentration of Hg^{2+}. The fluorescence intensity measurements were carried out at an emission wavelength of 347 nm. The limits of detection (LOD) and quantification (LOQ) of the developed method were determined to be 14.0 µM and 41.4 mg/L, respectively. The working range of the method was established between 35 and 95 µM. The proposed method was successfully applied to tap water and river water samples.

3. Results and discussion

3.1. Synthesis and characterization of CNDs

The summary of the hydrothermal method used for the synthesis of CNDs is shown in **Scheme 1**. The morphology of the CNDs was examined using transmission electron microscopy (TEM), which revealed the formation of aggregated clusters with sizes smaller than 50 nm (Fig. 1a). In the HRTEM images of the CNDs (Fig. 1b), a 0.34 nm d-spacing corresponding to the (002) plane of hexagonal graphite was observed, indicating that the CNDs possess a hexagonal graphite structure [25–27].

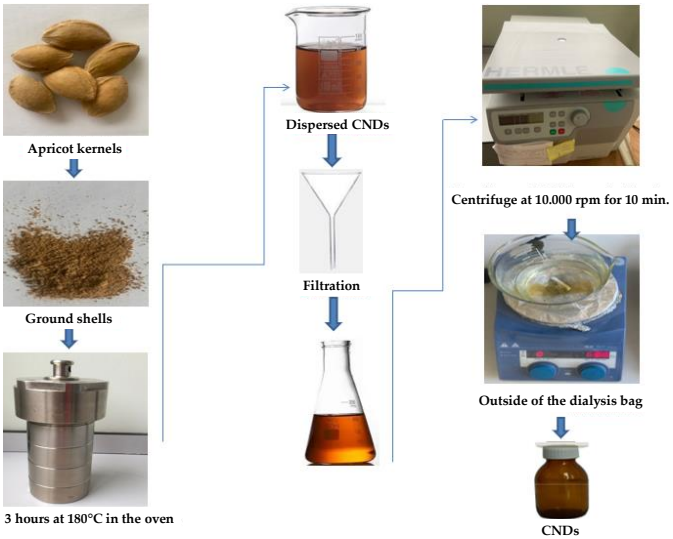

Scheme 1. Schematic diagram of the synthesis of CNDs via hydrothermal method

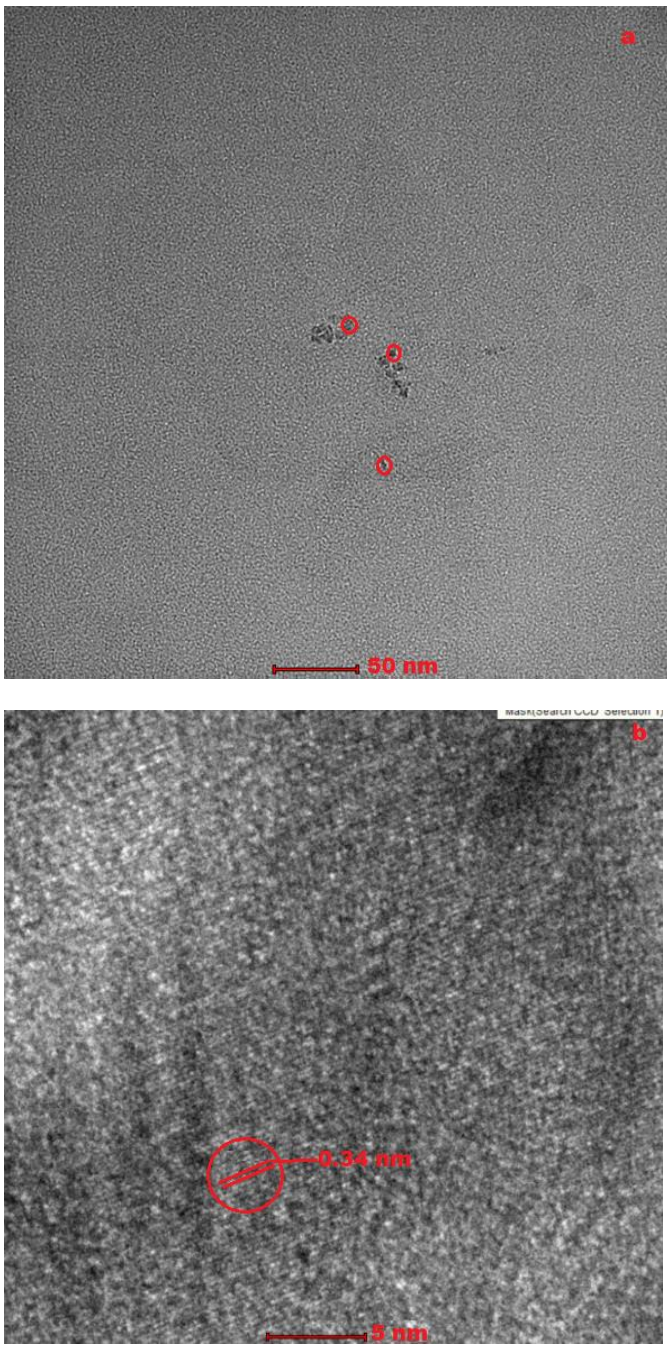

Figure 1. (a): TEM image of CNDs, **(b):** HRTEM image of CNDs

XRD analysis confirmed the presence of a graphite-like structure in CNDs (Fig. 2). The broad peak observed in the XRD pattern of the CNDs at approximately 2θ = 22.3° is characteristic of amorphous carbon structures [28]. This peak reflects the short-range ordering and partially crystalline nature of the CNDs. Additionally, this value corresponds to a d-spacing of around 0.4 nm, commonly observed in carbon materials such as amorphous carbon, carbon nanotubes, or graphene oxide [29]. This suggests that the CNDs do not exhibit a fully crystalline structure but instead display partial ordering and possess an amorphous character [30]. The peak observed at 2θ = 34.0° in the XRD pattern corresponds to the (112) planes of graphite, confirming that the CNDs possess a hexagonal graphite structure [31]. The crystallite size of the CNDs was approximately calculated to be 32.2 nm using the Scherrer equation based on the XRD data.

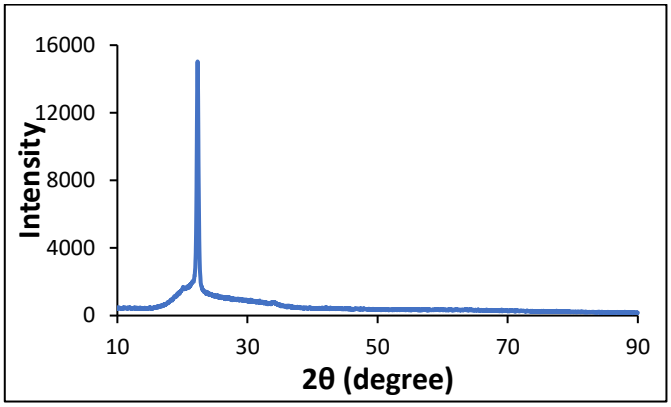

Figure 2. XRD diffractogram of CND

XPS analysis was employed to determine the elemental composition of the CNDs, identifying the presence of carbon, oxygen, and nitrogen atoms (Fig. 3a). A detailed deconvolution of the XPS spectra revealed that the C1s peak was associated with various carbon bonding environments, including C=C, C–C, C–O, and C–N bonds (Fig. 3b). The N1s peak was attributed to pyridinic C–N bonds, indicating the presence of nitrogen in a nitrogen-rich functional group (Fig. 3c). The O1s peak was assigned to a combination of oxygen-containing functional groups, including C=O, O–H, and C–O bonds (Fig. 3d), further confirming the presence of oxygen functionalities on the surface of the CNDs.

FTIR spectroscopy provided further evidence for the functional groups present within the structure of CNDs (Fig. 4). Substantial vibrational bands included the C–H stretching vibration at 2913 cm^{-1}, C=C stretching vibration at 1590 cm^{-1}, the O–H stretching vibration at 3311 cm^{-1}, the C=O stretching vibration at 1723 cm^{-1}, and the C–O/C–N stretching vibrations at 1029 cm^{-1}.

3.2. Optical and fluorescence properties of CNDs

The optical properties of CNDs were analyzed using UV-Vis absorption spectroscopy. The UV-Vis absorption spectrum of CNDs is presented in Fig. 5. A strong absorption peak observed around 200 nm is attributed to the $\pi \rightarrow \pi^*$ transitions of the C=C bonds, characteristic of sp^2-hybridized carbon atoms within the graphite-like structure. Additionally, an absorption band near 250 nm corresponds to $n \rightarrow \pi^*$ transitions of C–O and C–N bonds. These findings align with previously reported UV-Vis absorption spectra of carbon-based nanomaterials [32].

The visual appearance of the aqueous CND solution was documented under both daylight and UV light at 365 nm, as illustrated in **Fig. 5**.

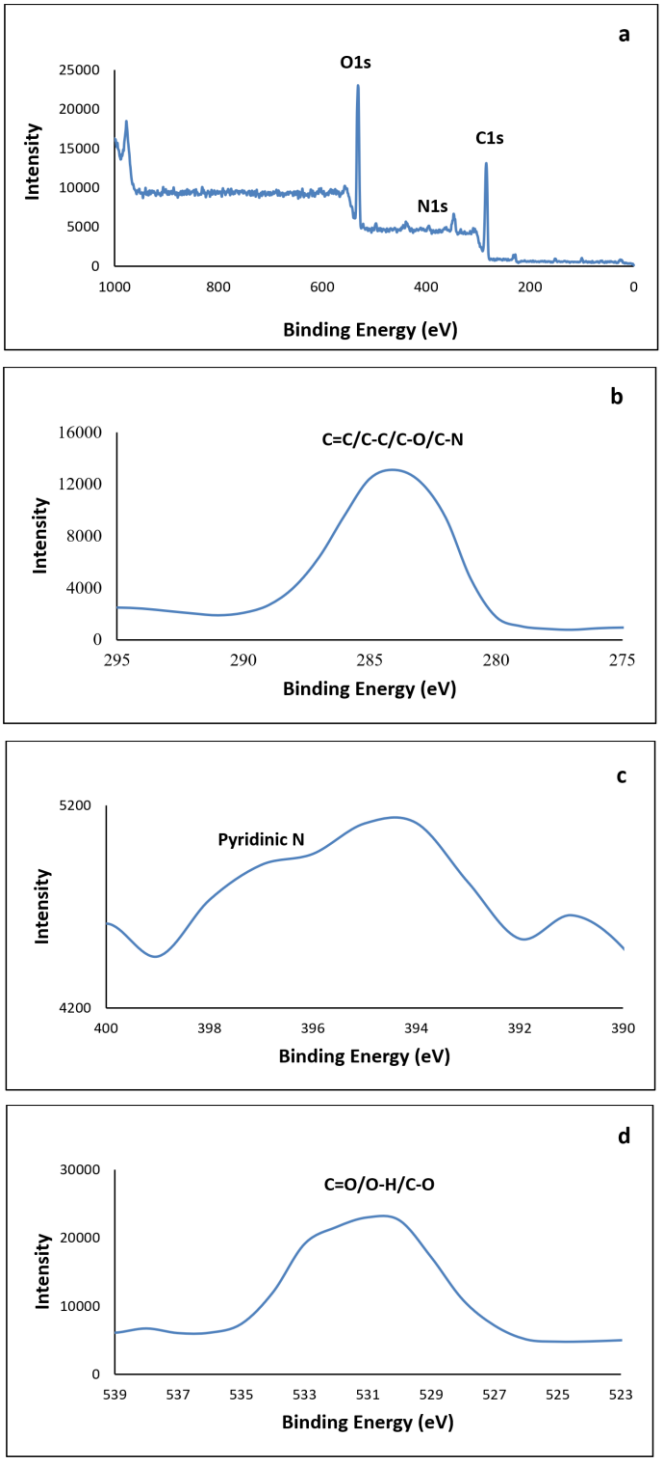

Figure 3. (a): XPS full spectra for the CNDs, **(b):** C1s, **(c):** N1s, **(d):** O1s spectra.

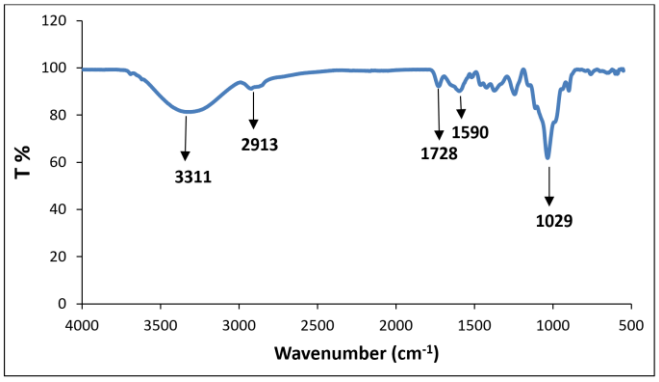

Figure 4. FTIR spectra of CNDs

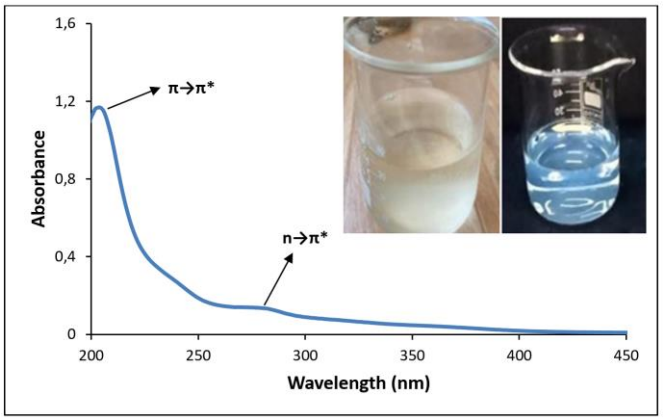

Figure 5. UV-Vis absorption spectrum of CNDs. Images of the CND solution under UV light (inset right) and daylight (inset left)

Under daylight conditions (Fig. 5 inset, left), the CND solution exhibited a pale yellow color, whereas under UV light (Fig. 5 inset, right), it displayed blue fluorescence. This observation confirms the fluorescent properties of the synthesized CNDs. The quantum yield of the CNDs was also determined using quinine sulfate as the standard reference. The quantum yield was found to be 0.27.

To further investigate the fluorescence properties of CNDs, fluorescence emission spectra of the aqueous CND solution were recorded at excitation wavelengths ranging from 300 to 400 nm in 10 nm intervals (Fig. 6). As depicted in Fig. 6, increasing the excitation wavelength resulted in a decrease in fluorescence emission intensity and a red shift in the emission peak maxima. This excitation-dependent fluorescence behavior demonstrates that the synthesized CNDs exhibit multicolor fluorescence characteristics, consistent with findings reported in the literature [32]. As shown in Fig. 6, the CNDs exhibited the highest fluorescence intensity when excited at 310 nm. Therefore, 310 nm was used as the excitation wavelength in subsequent studies.

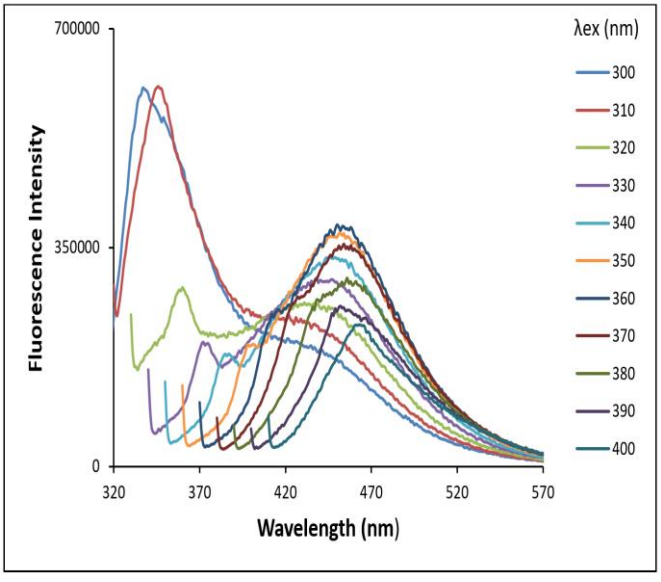

Figure 6. Emission spectra of CNDs at different excitation wavelengths

3.3. The effect of pH on the fluorescence intensity of CNDs

The fluorescence intensity of CNDs is highly influenced by pH, and this effect has been extensively studied in the literature [13]. To examine the effect of pH on the fluorescence intensity of prepared CNDs, solutions of CNDs were prepared across a pH range of 3 to 11 and excited at 310 nm. Fluorescence intensity at 347 nm was subsequently recorded, as shown in Fig. 7. As depicted, a significant reduction in fluorescence intensity is observed at pH 11, while no notable changes in fluorescence intensity occur at pH values of 3, 5, and 7. Considering that the pH of real samples typically ranges around 7, the experiments were conducted without the addition of any buffer solution. This approach, which eliminates the need for supplementary chemicals, provides several advantages, including cost-effectiveness, environmental sustainability, and a more efficient experimental procedure. These benefits make this method a more practical and efficient alternative compared to other Hg^{2+} detection techniques reported in the literature.

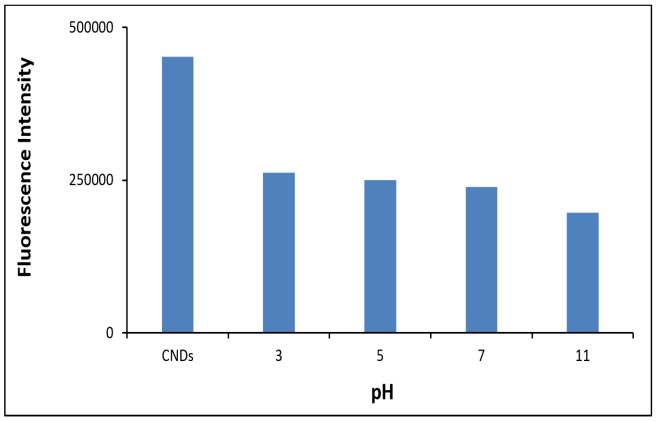

Figure 7. Variation of the fluorescence intensity of CNDs with pH (λ_{ex}:310 nm, λ_{em}:347 nm)

3.4. The effect of cations on the fluorescence of CNDs

The interactions between CNDs and a variety of cations were systematically investigated by monitoring the fluorescence response at an excitation wavelength of 310 nm. The effect of 36 different cations on the fluorescence spectra of CNDs was explored, including Li^{+}, Na^{+}, K^{+}, Be^{2+}, Mg^{2+}, Ca^{2+}, Sr^{2+}, Ba^{2+}, Sc^{3+}, Y^{3+}, Ti^{4+}, V^{5+}, Cr^{3+}, Mo^{6+}, W^{6+}, Mn^{2+}, Fe^{3+}, Co^{2+}, Ni^{2+}, Cu^{2+}, Ag^{+}, Zn^{2+}, Cd^{2+}, B^{3+}, Al^{3+}, Tl^{+}, As^{5+}, Se^{2+}, NH_4^{+}, Au^{3+}, Sb^{3+}, Sn^{4+}, Bi^{3+}, Hg^{2+}, Pd^{2+}, and Pb^{2+} (Fig. 8a). Changes in the fluorescence intensity of CNDs upon interaction with different cations were monitored to evaluate their binding affinity and selectivity. This analysis aimed to elucidate the selectivity of CNDs for particular cations, with a focus on those ions that induced the most pronounced changes in fluorescence behavior.

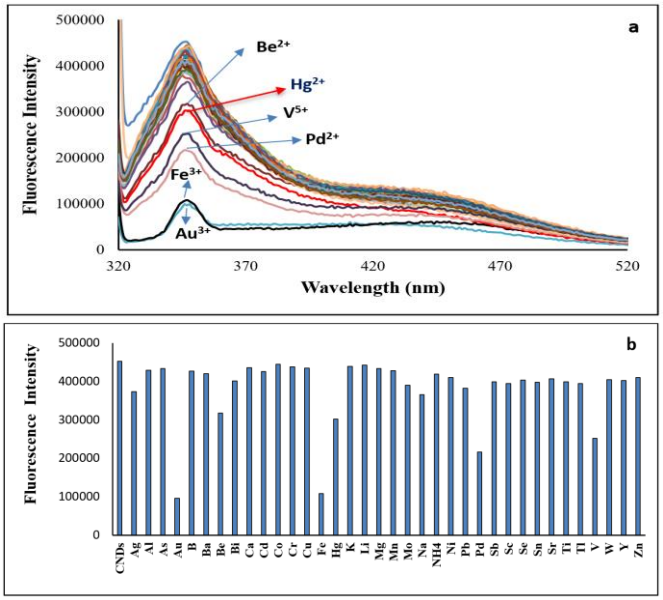

Figure 8. (a): Effect of cations on the fluorescence spectrum of CND, **(b):** The changes in fluorescence intensity at 347 nm with the effect of cations

Fig. 8a illustrates the effect of various cations on the fluorescence spectrum of CNDs. Upon analyzing the interaction results, notable quenching in fluorescence intensity was observed with Be^{2+}, V^{5+}, Fe^{3+}, Au^{3+}, Hg^{2+}, and Pd^{2+} cations (Fig. 8b). Spectrofluorimetric titrations were performed to determine whether the fluorescence quenching was related to the concentration of cation. However, there were no consistent and reproducible fluorescence responses with the increasing concentrations of Be^{2+}, V^{5+}, Fe^{3+}, Au^{3+}, and Pd^{2+} ions. The regular and predictable fluorescence quenching observed with only increasing Hg^{2+} concentrations provided a reliable basis for continued studies to develop a sensitive and selective determination method. Fig. 9 demonstrates the consistent fluorescence quenching in the spectra of CNDs as the concentration of Hg^{2+} increases. The inset of Fig. 9 illustrates the correlation between the fluorescence intensity at 347 nm and the Hg^{2+} concentration. A regular fluorescence quenching effect was observed within the Hg^{2+} concentration range of 35 to 95 µM (Fig. 9 inset).

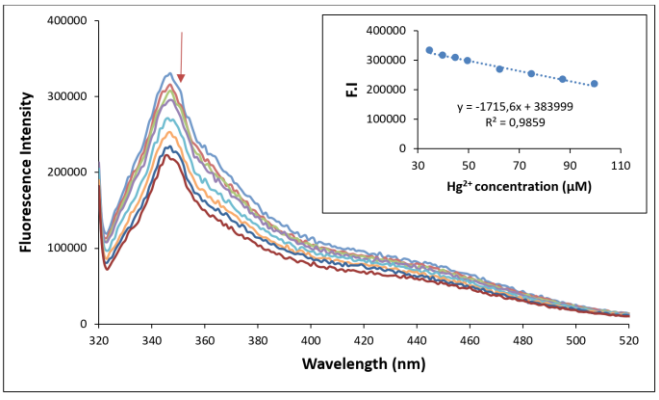

Figure 9. Spectrofluorimetric titration of CNDs with Hg^{2+} ions. Inset: Regular quenching in the fluorescence intensity of CNDs at 347 nm with increasing Hg^{2+} concentration (Hg^{2+} concentration: 35-95 µM)

3.5. Determination of Hg^{2+} ions

The determination of Hg^{2+} was performed using the standard calibration method. The analytical performance data of the proposed method is presented in Table 1. The LOD and LOQ values of the method were determined to be 14.0 µM and 41.4 µM, respectively. The linear range (LR) was established to be 35-95 µM. The accuracy of the method was demonstrated through spiking-recovery studies conducted on real water samples. The results are presented in Table 2. As shown in Table 1, the correlation coefficient was 0.9859, indicating a high degree of linearity. The LOD value was calculated by dividing three times the standard deviation by the slope of the calibration curve. Eleven blank measurements were performed to determine the standard deviation for these experiments. The LOQ value was determined as three times the LOD.

Table 1. Analytical performance data of the proposed method for Hg^{2+} determination

Excitation wavelength (nm)	310
Emission wavelength (nm)	347
LOD (µM)	14.0
LOQ (µM)	41.4
LR (mg/L)	35-95
Fluorescent reagent	(8/10) diluted CND solution
Volume of CND solution (mL)	2
Total volume (mL)	4
Solvent	water
Pre-measurement time	1-2 min
Correlation coefficient (R^2)	0.9859

Table 2. Results of spiked-recovery experiments for Hg^{2+} determination in water samples (N=3)

Sample	Spiked Hg^{2+} (mg/L)	R%(intra-day)	R% (inter-day)
Deionized water	9.0	96.2±1.2	95.1±1.5
Tap water	9.0	97.8±1.4	96.3±1.3
River water	9.0	97.8±0.9	95.9±1.1

3.6. Quenching mechanism

The Stern-Volmer relationship can be used to explain the fluorescence quenching of CNDs in the presence of Hg^{2+}. In the Stern-Volmer equation given by Eq. (2), Ksv represents the Stern-Volmer quenching constant, while I_0 and I denote the fluorescence intensities in the absence and presence of the quencher (Hg^{2+}), respectively. [Q] symbolizes the molar concentration of the quencher.

$$I_0/I = 1 + Ksv\,[Q] \quad (2)$$

As expected from Eq. 2, plotting I_0/I versus the molar concentration of the quencher should yield a straight line with a y-axis intercept of 1 when the quenching mechanism follows the Stern-Volmer relationship. The slope of this line corresponds to K_{sv}. The static quenching mechanism is based on the complexation of the quencher with the fluorophore in the ground state, while dynamic quenching is generally associated with collisions in the excited state [33]. The Stern-Volmer equation remains valid for both quenching processes, despite the differing mechanisms. Fig. 10a presents the Stern-Volmer plot for Hg^{2+}-induced fluorescence quenching of the CNDs. As seen in Fig. 10a, the intercept of the line on the y-axis is 1. This indicates that the Stern-Volmer relationship is valid for this system. However, to determine whether the quenching is dynamic or static, the effect of temperature was investigated. Fig. 10b shows the effect of temperature on I_0/I. As seen in Fig. 10b, the I_0/I value increases with increasing temperature. This result suggests that the quenching occurs through dynamic quenching [33].

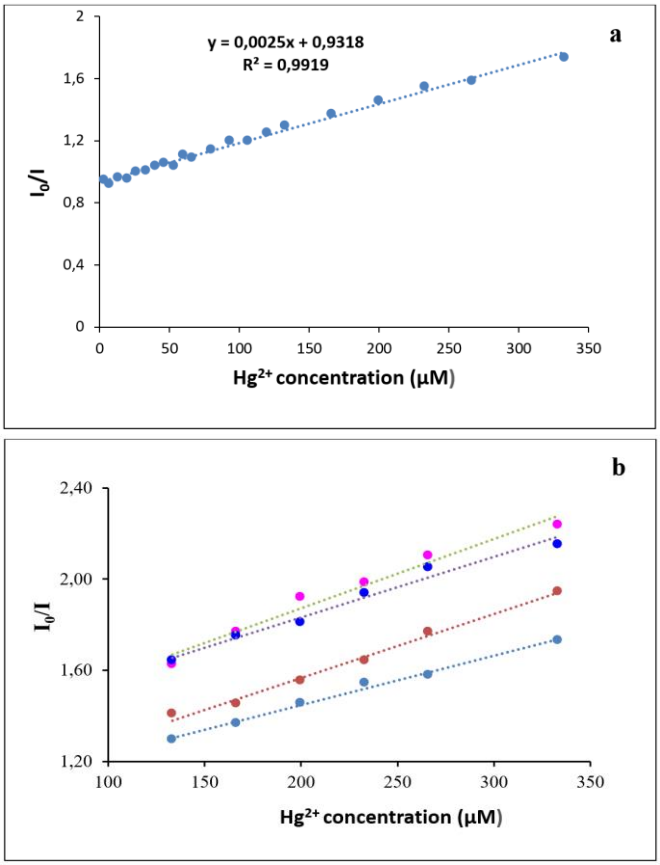

Figure 10. Stern-Volmer plot. The light blue: 297 K, the orange: 313 K, and the dark blue: 353 K

3.7. Comparison with other CNDs

Table 3 summarizes a comparison of several spectrofluorimetric Hg^{2+} detection methods in water samples based on CNDs reported in the literature. As shown in Table 3, although the LOD and LR values of these methods are more advantageous compared to the proposed work, the CNDs used as fluorescent probes in these studies were generally synthesized using chemical sources of carbon, such as ammonium citrate, citric acid, folic acid, ethylene glycol, and urea [18,34,36,37]. In contrast, in the presented study, apricot seed shells were utilized as a carbon source, making it a green synthesis approach compared to the methods in the literature.

Table 3. Comparison of CNDs-based methods for Hg^{2+} detection in water in the literature

Fluorescent reagent	Carbon source	Reaction temp. time	Chemicals	Sample	LOD (μM)	LR (μM)	Ref.
CDs	Folic acid, ethylene glycol	180 °C, 12h	—	Lake water, tap water	0.23	0-25	34
CDs	Carbon target	71h	HNO_3, PEG200, N-acetyl-l-cysteine, ethyl acetate	—	—	0-2.69	35
NSCNDs	Citric acid/urea/Lcysteine	MW, 5 min.	—	Lake water, tap water	2	0-40	36
CDs	Ethylene glycol	140 °C, 6h	H_2SO_4	Tap water	0.035	0-1	37
FCDs	Citric acid	180 °C, 10h	NaOH, $NaBH_4$	Tap water	0.02	0.1-1.2	13
NCDs	Ammonium citrate, urea	180 °C, 5h	—	Tap water	0.045	0.05-24.9	18
CQDs	Medlar Seed	300 °C, 2h	—	Tap, sea, and stream water	1.3	4.9-24.9	38
CNDs	Apricot kernel shells	180 °C, 3h	—	Tap water, river water	14	35-95	This work

Additionally, the methods in the literature involve relatively long reaction times [18,34,35, 37,13]. However, the reaction time in the proposed study is much shorter than most of the reaction times reported in the literature. Namely, the proposed synthesis method is a fast approach. As seen in Table 3, toxic chemicals such as NaOH and H_2SO_4 were used in some stages of the synthesis processes reported in the literature [37, 13]. In contrast, in the proposed study, only apricot seed shells, a natural waste product, were used as the carbon source in the hydrothermal synthesis of CNDs. Therefore, the proposed method is an environmentally friendly and cost-effective approach. The method was successfully applied to the determination of Hg^{2+} in tap water and river water samples. These results demonstrate that the proposed method is a rapid, economical, and environmentally friendly approach that can be effectively applied to water samples containing Hg^{2+} at concentrations within the detection limits of the method.

4. Conclusion

CNDs were efficiently synthesized from apricot kernel shells using a green hydrothermal synthesis method. The synthesized CNDs were characterized by TEM, XRD, XPS, and FTIR spectroscopy. The optical properties of the CNDs were analyzed using UV-vis absorption and fluorescence spectroscopy. The method demonstrated a linear range for Hg^{2+} detection between 35 and 95 μM. The LOD and LOQ values were determined to be 14 μM and 41.4 μM, respectively. The accuracy of the proposed method was successfully validated in tap water and river water samples.

In conclusion, the proposed spectrofluorimetric method provides a rapid, cost-effective, and highly selective approach for the detection of Hg^{2+} in water samples. By utilizing CNDs synthesized from apricot kernel powder, this method offers a significant improvement over existing techniques reported in the literature. It presents an eco-friendly and highly selective alternative for environmental monitoring and analytical applications, demonstrating both practical and environmental advantages.

Author contributions:

Najlaa Ayad Salahaldeen, Nurhayat Özbek, Ümmühan Turgut Ocak, and Miraç Ocak wrote the main manuscript text and prepared all figures. All authors reviewed the manuscript.

Funding:

No funding.

Data availability:

Datasets and materials used can be reached from Najlaa Ayad Salahaldeen.

Declarations

Competing interests:

The authors declare no competing interests.

Ethical approval:

An ethics approval is not legally required for the study.

References

[1] D.S. Chauhan, MA. Quraishi, C. Verma, Carbon nanodots: recent advances in synthesis and applications, Carbon Lett, 32, 2022, 1603–1629.

[2] S. Dinç, M. Kara, Synthesis and applications of carbon dots from food and natural products: Review, J Api Nat, 1, 2018, 33–37.

[3] M. Jabeen, I. Mutaza, A comprehensive review on carbon quantum dots, Turk J Anal Chem 6, 2024, 50–60.

[4] X. Sun, Y. Lei, Fluorescent carbon dots and their sensing applications, TrAC Trends Anal Chem, 87, 2017, 163–180.

[5] WL. Zhong, JY. Yang, Fluorescent carbon quantum dots for heavy metal sensing, Sci Total Environ, 957, 2024, 177473.

[6] G. Bjørklund, M. Dadar, J. Mutter, J. Aaseth, The toxicology of mercury: Current research and emerging trends. Environ Res, 159, 2017, 545–554.

[7] A. Kumar, V. Kumar, P. Bakshi, RD. Parihar, M. Radziemska, R. Kumar, Mercury in the natural environment: Biogeochemical

cycles and associated health risks, J Geochem Explor 267, 2024, 107594.
[8] M.V. Maia, WT. Suarez, V. Bezerra dos Santos, SC. Bezerra de Oliveira, JP. Barbosa de Almeida, A novel approach to Hg^{2+} determination in water samples using carbon dots based on paper and fluorescence digital image analysis, J Chem Technol Biotechnol, 99, 2024, 1157–1164.
[9] DJ. Dai, CY. Zhang, NT. Thi Dieu Thuy, G. Zhao, W. Lu, JY. Fan, Strong fluorescence quenching of carbon dots by mercury (II) ions: Ground-state electron transfer and diminished oscillator strength, Diam Relat Mater, 126, 2022, 109076.
[10] J.Y. Liang, L. Han, SG. Liu, YJ. Ju, NB. Li, HQ. Luo, Carbon dots-based fluorescent turn off/on sensor for highly selective and sensitive detection of Hg^{2+} and biothiols. Spectrochim Acta A: Mol Biomol Spectrosc, 222, 2019, 117260.
[11] E. Yahyazadeh, F. Shemirani, Easily synthesized carbon dots for determination of mercury (II) in water samples, Heliyon 5, 2019, e01596.
[12] PY. Yin, GX. Yao, TR. Zou, N. Na, WR. Yang, HB. Wang, W. Tan, Facile preparation of N, S co-doped carbon dots and their application to a novel off-on fluorescent probe for selective determination of Hg^{2+}, Dyes Pigments, 206, 2022, 110668.
[13] ZH. Gao, ZZ. Lin, XM. Chen, ZZ. Lai, ZY. Huang, Carbon dots-based fluorescent probe for trace Hg^{2+} detection in water sample, Sens Actuators B Chem, 222, 2016, 965–971.
[14] S. Samota, P. Tewatia, R. Rani, S. Chakraverty, A. Kaushik, Carbon dot nanosensors for ultra-low level, rapid assay of mercury ions synthesized from an aquatic weed, Typha angustata Bory (Patera), Diam Relat Mater, 130, 2022, 109433.
[15] KHH. Aziz, KM. Omer, RF. Hamarawfa, Lowering the detection limit towards nanomolar mercury ion detection via surface modification of N-doped carbon quantum dots, New J Chem, 4, 2019, 8677–8683.
[16] L.K. Singh, S. Sharma, K.K. Ghosh, Spectroscopic detection of Hg^{2+} in water samples using fluorescent carbon quantum dots as sensing probe, Main Group Chem, 20, 2021, 1–18.
[17] D. Huang, CG. Niu, M. Ruan, X.Y. Wang, G.M. Zeng, C.H. Deng, Highly sensitive strategy for Hg^{2+} detection in environmental water samples using long lifetime fluorescence quantum dots and gold nanoparticles, Environ Sci Technol, 47, 2013, 4392–4398.
[18] Y. Zhang, N. Jing, JQ. Zhang, YT. Wang, Hydrothermal synthesis of nitrogen-doped carbon dots as a sensitive fluorescent probe for the rapid, selective determination of Hg^{2+}, Int J Environ Anal Chem, 97, 2017, 841–853.
[19] H.H. Jing, F. Bardakci, S. Akgöl, K. Kusat, M. Adnan, M.J. Alam, R. Gupta, S. Sahreen, Y. Chen, S.C.B. Gopinath, S. Sasidharan, Green Carbon Dots: Synthesis, characterization, properties and biomedical applications, J Funct Biomater, 14, 2023, 27.
[20] H.B. Xu, S.H. Zhou, M.Y. Li, P.R. Zhang, Z.H. Wang, Y.M. Tian, X.Q. Wang, Preparation of biomass-waste-derived carbon dots from apricot shell for highly sensitive and selective detection of ascorbic acid, Chinese J Anal Chem, 50, 2022, 100168.
[21] Z.Q. Zhang, C.H. Zhou, J.M. Yang, B.J. Yan, J.H. Liu, S.N. Wang, Q. Li, M.M. Zhou, Preparation and characterization of apricot kernel shell biochar and its adsorption mechanism for atrazine, Sustainability, 14, 2022, 4082.
[22] G. Predeanu, V. Slăvescu, M.F. Drăgoescu, N.M. Bălănescu, A. Fiti, A. Meghea, P. Samoila, V. Harabagiu, M. Ignat, A.M. Manea-Saghin, BS. Vasile, N. Badea, Green synthesis of advanced carbon materials used as precursors for adsorbents applied in wastewater treatment, Materials (Basel), 16, 2023, 1036.
[23] S.D. Torres Landa, N.K. Bogireddy, I. Kaur, V. Batra, V. Agarwal, Heavy metal ion detection using green precursor derived carbon dots, iScience, 25, 2022, 103816.
[24] F. Li, C.J. Liu, J. Yang, Z. Wang, W.G. Liu, F. Tian, Mg/N double doping strategy to fabricate extremely high luminescent carbon dots for bioimaging, RSC Adv, 4, 2014, 3201–3205.
[25] D. Ozyurt, M. Al Kobaisi, R.K. Hocking, B. Fox, Properties, synthesis, and applications of carbon dots: A review, Carbon Trends, 12, 2023, 100276.
[26] N.C. Verma, A. Yadav, C.K. Nandi, Paving the path to the future of carbogenic nanodots, Nat Commun, 10, 2019, 2391.
[27] C.J. Reckmeier, J. Schneider, A.S. Susha, AL. Rogach, Luminescent colloidal carbon dots: optical properties and effects of doping, Opt Express, 24, 2016, A312-A340.
[28] B. Ramoğlu, A. Gümrükçüoğlu, E. Çekirge, M. Ocak, Ü. Ocak, One spot microwave synthesis and characterization of nitrogen doped carbon dots with high oxygen content for fluorometric determination of banned Sudan II dye in spice samples, J Fluoresc, 31, 2021, 1587-1598.
[29] A.B. Siddique, A.K. Pramanick, S. Chatterjee, M. Ray, Amorphous carbon dots and their remarkable ability to detect 2,4,6-trinitrophenol, Sci R*ep*, 8, 2018, 9770.
[30] M. Kavgacı, HV. Kalmış, H. Eskalen, Synthesis of fluorescent carbon quantum dots with hydrothermal and solvothermal method application for anticounterfeiting and encryption, Int J Inn Eng Appl, 7, 2023, 32-38.
[31] W.K. Zhang, Y.Q. Liu, X.R. Meng, T. Ding, Y.Q. Xu, H. Xu, Y.R. Ren, B.Y. Liu, J.J. Huang, J.H. Yang, XM. Fang, Graphenol defects induced blue emission enhancement in chemically reduced graphene quantum dots, Phys Chem Chem Phys, 17, 2015, 22361–22366.
[32] Y.P. Sun, B. Zhou, Y. Lin, W. Wang, K.A.S. Fernando, P. Pathak, M.J. Meziani, B.A. Harruff, X. Wang, P.G. Luo, H. Yang, M..E. Kose, B. Chen, LM. Veca, S.Y. Xie, Quantum-sized carbon dots for bright and colorful photoluminescence, Am Chem Soc, 128, 2006, 7756–7757.
[33] Y. Çağlar, E.T. Saka, H. Alp, H. Kantekin, M. Ocak, Ü. Ocak, A simple spectrofluorimetric method based on quenching of a Nickel(II)-phthalocyanine complex to determine iron (III), J Fluoresc, 26, 2016, 1381–1389.
[34] R. Zhang, W. Chen, Nitrogen-doped carbon quantum dots: Facile synthesis and application as a "turn-off" fluorescent probe for detection of Hg^{2+} ions, Biosens Bioelectron, 56, 2014, 83–90.
[35] H.M.R. Gonçalves, A.J. Duarte, J.C.G. Esteves Da Silva, Optical fiber sensor for Hg (II) based on carbon dots, Biosens Bioelectron, 4, 2010, 1302–1306.
[36] L. Li, B. Yu, T. You, Nitrogen and sulfur co-doped carbon dots for highly selective and sensitive detection of Hg (II) ions, Biosens Bioelectron, 74, 2015, 263–269.
[37] Y. Liu, C. Liu, Z. Zhang, Synthesis of highly luminescent graphitized carbon dots and the application in the Hg^{2+} detection, Appl Surf Sci, 258, 2012, 481–485.
[38] N. Özbek, E. Çekirge, M. Ocak, Ü. Ocak, Highly Blue-fluorescent Carbon Quantum Dots Obtained from Medlar Seed for Hg^{2+} Determination in Real Water Samples, J Fluoresc, 34, 2024, 2533–2542.